British Journal of Applied Science & Technology
16(1): 1-12, 2016, Article no.BJAST.26301
ISSN: 2231-0843, NLM ID: 101664541

SCIENCEDOMAIN *international*
www.sciencedomain.org

Quantitative Design and Evaluation of EMI Filters in a Digitally Controlled Boost PFC Converter

C. T. Ma[1*], B. H. Yao[1], F. Y. Chang[1], K. F. Chen[2] and Y. L. Chen[2]

[1]Department of EE, Applied Power Electronics Systems Research Group, College of EECS, National United University, Miaoli City 36063, Taiwan, R.O.C.
[2]Missile and Rocket Systems Research Division, National Chung-Shan Institute of Science and Technology, Taoyuan City 32546, Taiwan, R.O.C.

Authors' contributions

This work was carried out in collaboration between all authors. The first author CTM led on the study, performed the theoretical analysis, evaluated the method and wrote the first draft of the manuscript. Authors BHY and FYC are postgraduate students, managed the figures, waveforms and literature searches. Authors KFC and YLC provided discussions in preparation of the paper. All authors read and approved the final manuscript.

Article Information

DOI: 10.9734/BJAST/2016/26301
Editor(s):
(1) Rodolfo Dufo Lopez, Electrical Engineering Department, University of Zaragoza, Spain.
Reviewers:
(1) Prashant Kumar, Savitribai Phule Pune University, India.
(2) Jayalakshmi N. Sabhahit, Manipal University, Manipal, India.
Complete Peer review History: http://sciencedomain.org/review-history/14593

Original Research Article

Received 9th April 2016
Accepted 5th May 2016
Published 12th May 2016

ABSTRACT

This paper presents a quantitative design procedure for electromagnetic interference (EMI) filters and investigates the effectiveness of the designed EMI filters in a digitally controlled boost power factor correction (PFC) converter. In most modern electrical equipment, the problem of low power factor due to their intrinsic impedance characteristics has greatly reduced the efficiency of using electric energy. In order to improve the quality of electric power supply while achieving the goal of energy conservation, high-power converters tend to use an active PFC circuit as their front stage connecting to the mains. However, active PFC circuits which utilize high-frequency switching techniques in tracking input line currents often bring EMI and harmonic distortion problems to distribution systems. To ensure that the equipment can meet the relevant EMI standards, some properly designed EMI filters must be used to reduce the common mode and differential mode noises. Due to inevitable nonlinear interactions of the EMI filter and the PFC bridge rectifier, the

**Corresponding author: E-mail: ctma@nuu.edu.tw;*

EMI filter is normally designed by repeated trial-and-errors in practice. To improve the design efficiency, this paper firstly introduces a single-switch boost PFC circuit widely used in various ac-dc converters along with the proposed systematic design procedure for EMI filters and followed by simulation analysis in PSIM software environment. Finally, a 1 kW digitally controlled boost PFC converter prototype with the designed EMI filter is practically constructed and tested to verify the effectiveness of the proposed design method.

Keywords: Power quality; power factor correction; switching power supply; electromagnetic interference filter.

1. INTRODUCTION

In conventional AC-DC power converters, a full bridge rectifier paralleled with a filtering capacitor is normally used to obtain a desired front-end DC voltage. Because of the nonlinear characteristics exhibited in the full-bridge rectifier and its filtering devices there is always a phase shift between the voltage and input current resulting in lower power factor and high current harmonic distortion [1]. In order to improve these problems, most medium to high power AC-DC converters utilize a power factor correction (PFC) module which is designed to achieve the required front-end DC voltage, to shape the input current of the power converter to be in synchronization with the mains voltage and to maximize the real power drawn from the mains [2,3]. From a theoretical point of view, an ideal PFC module must be able to regulate its output DC voltage, to force the input current to follow the input voltage just like the case of connecting a pure resistive load and these must be done without any input current harmonics [4]. Although the above mentioned PFC functions and features can be realized with passive or active circuits, advanced AC-DC converters tend to use active PFC circuits to meet the increasingly rigorous power quality standards and improve the overall quality of electric power supply system [5-8]. However, active PFC circuits which utilize high-frequency switching method in tracking input line currents often bring EMI and harmonic distortion problems to distribution systems [9-11]. To solve the above problems, a properly designed EMI filter and suitable PFC control techniques must be used [12-14]. Of the international power quality and EMI standards, the most important ones for harmonic distortions in switching-mode power supply are EN-61000 [15] and IEEE-1547 [16] and the standards for EMI are EN-55022 [17] and FCC part 15B [18].

In the open literature, fundamental research results regarding the design of EMI filters and current harmonic distortion issues in switching-mode power converters have been published [19]. More recently, issues regarding PFC topology and stability analysis of EMI filters are discussed in [20,21]; however, since the complex relationship between harmonic distortions and the EMI filter parameters are not yet clearly understood, a general engineering design procedure for finding a suitable EMI filter on a specific design case is still call for development. The contribution of this paper is to provide a simple and effective design guideline for EMI filters. In this paper, a simple step by step procedure for designing EMI filters is proposed and the performance of eliminating harmonic currents is optimized in a digitally controlled boost PFC circuit. In the design case presented in this paper, the harmonic distortion is quantitatively evaluated after the parameters of EMI filter have been obtained. Because the design of a boost PFC circuit involves many different practices and topologies this paper firstly introduces a single-switch boost PFC circuit widely used in various ac-dc converters. The related EMI sources and their equivalent circuits in the boost PFC circuit are then analyzed along with the proposed systematic design procedure for EMI filters and followed by some simulation analysis in PSIM software environment. Finally, a DSP controlled 1 kW boost PFC prototype integrated with the designed EMI filter is constructed and some experimental tests are carried out to verify the effectiveness of the proposed design methods.

2. POWER FACTOR CORRECTION CIRCUIT TOPOLOGY

2.1 PFC Topologies and Operating Modes

Theoretically, the function of PFC be achieved by several topologies, the boost converter is the most popular topology used in various applications. This is because the boost PFC converter can be operated in three modes; i.e., continuous conduction mode (CCM), discontinuous conduction mode (DCM), and

critical conduction mode (CRM). Fig. 1 shows the PFC circuit topology and the conceptually modeled waveforms to illustrate the inductor and input currents in the three operating modes.

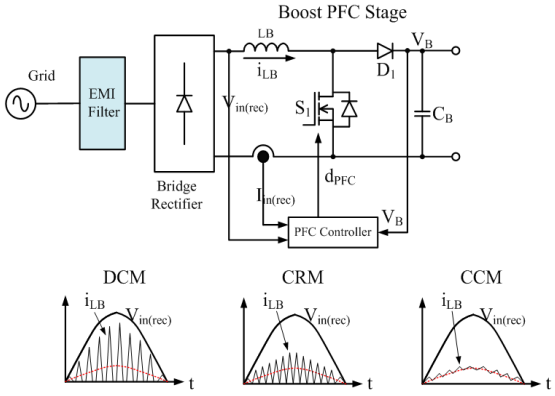

Fig. 1. The topology and waveforms of a boost PFC converter

For low power applications, the CRM boost has some advantages in power saving and higher power density; however when the power level is increased the low filtering feature and the high peak current starts to appear and the CCM operation become a better choice for high power applications. Since this paper is intended to investigate EMI design issues in medium to high power PFC applications, a CCM PFC boost converter is chosen for the detailed EMI filter design discussions and a design example for demonstration via simulations and measurements on a digitally controlled 1 kW hardware prototype.

2.2 Control of a Boost PFC Converter

For a PFC boost converter operating in CCM, the dual loop control structure as shown in Fig. 2 is the most commonly used in medium to high power applications. In Fig. 2, the Kv and Ks are the factors of voltage and current sensors. The feedback signal of the output voltage (Vdf) is compared with the desired reference voltage (Vd*) and operated by an error amplifier to get the signal of Vea, The Vea signal is then multiplied by the sensed input voltage signal (KvVin(rec)) to produce the inductor current command, Is*. The Is* are compared with the feedback inductance current signal (Is) and get through the inner loop error amplifier (G_{CA}) to finally obtain the PWM control signals, Vcon and the duty of the power switch. The two error amplifiers, G_V and G_{CA}, used in Fig. 2 are all type-II compensators to achieve a satisfactory performance.

From Fig. 2, the voltage of the boost inductor can be expressed as:

$$L\frac{dI_{in}}{dt} = V_{in} - (1-d)V_o \tag{1}$$

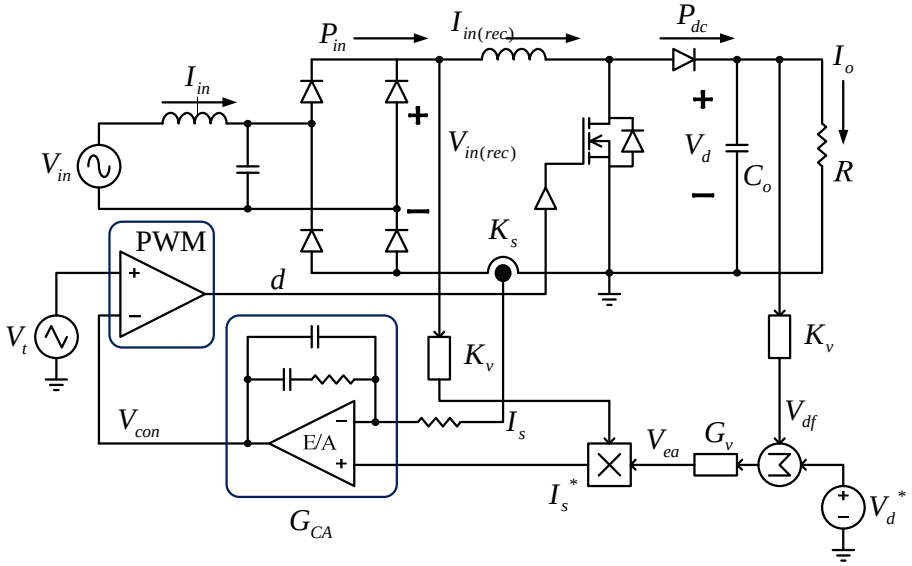

Fig. 2. The dual loop control structure of a CCM boost PFC

The small signal model of (1) can be obtained by using linearlization techniques as shown in (2) and the transfer function of inductor current can then be derived as shown in (3).

$$\frac{\tilde{I}_{in}}{\tilde{d}} = \frac{V_o}{sL} \tag{2}$$

$$H = \frac{\tilde{I}_s}{\tilde{V}_{con}} = \frac{\tilde{I}_{in} K_s}{\tilde{d} V_s} = \frac{K_s V_o}{sLV_s} \tag{3}$$

Using (3), the inner loop current controller can be designed as follows:

$$G_{ca} = \frac{K_1 (s + F_z)}{s(s + F_p)} \tag{4}$$

The overall control block diagram of the PFC inner loop current controller is shown in Fig. 3. Using the power balance concept, i.e., the input real power of the PFC module equal to its output DC power plus the system losses assuming that unity power factor is achieved, the same design method can then be applied to the design of outer loop voltage regulator of the boost PFC as shown in (7). The overall control block diagram of the PFC outer loop voltage controller is shown in Fig. 4.

$$\frac{V_O}{V_{ea}} = \frac{k_{dcf}}{sC} \tag{5}$$

$$H_{voltage} = \frac{v_o}{V_{ea}} = \frac{k_{dcf} K_{vo}}{sC} \tag{6}$$

$$G_v = \frac{K_2 (s + F_z)}{s(s + F_p)} \tag{7}$$

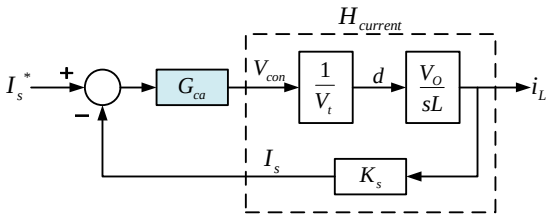

Fig. 3. The overall control block diagram of the PFC inner loop current controller

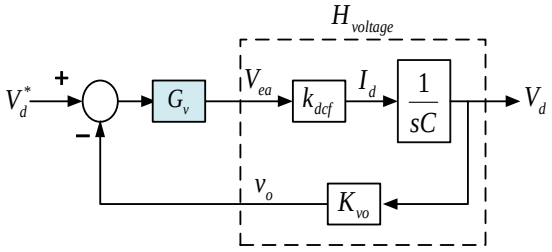

Fig. 4. The overall control block diagram of the PFC outer loop voltage controller

3. THE ELECTROMAGNETIC INTERFERENCE IN PFC AND ITS SPECIFICATIONS

3.1 Source of Conducted EMI Noises

In an active PFC circuit, EMI noise normally includes common-mode and differential mode noises. Fig. 5 shows the signal paths of the above common-mode and differential-mode currents with a line impedance stabilization network (LISN), an important interfacing circuit for practically measuring the conductivity electromagnetic interference in PFC circuits. In a single-phase three-wire AC power system, the noise currents can be separated into two parts according to their flow into the common mode current and the differential-mode noise current. The common-mode noise currents, $\tilde{I}_{CM}$, have two loops, i.e. the line (L) and neutral(N) to the ground (G), while the differential mode noise current, $\tilde{I}_{DM}$, is flowing the loop between (L) and (N).

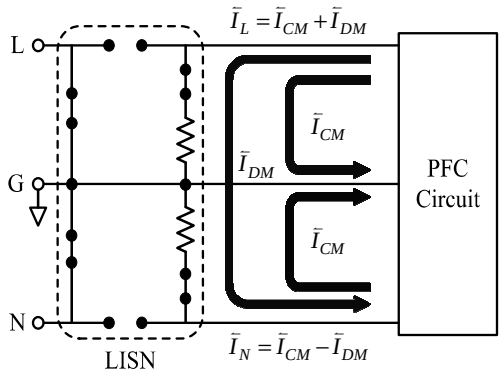

Fig. 5. The signal paths of the common-mode and differential-mode currents with a line impedance stabilization network (LISN)

From Fig. 5, it is easy to calculate the noise currents flowing on the line and neutral as follows:

$$\bar{I}_L = \bar{I}_{CM} + \bar{I}_{DM} \quad (8)$$

$$\bar{I}_N = \bar{I}_{CM} - \bar{I}_{DM} \quad (9)$$

In order to design an EMI filter which is able to effectively suppress possible noises produced by the active PFC circuit, investigating the possible noise sources and their coupling paths is very important [9,10]. The common mode noise current in the studied boost PFC circuit is mainly composed by high frequency transient voltage of the switching element or those circuit parasitic capacitances (C_p, C_{g1}, C_{g2}) formed by the charge and discharge currents. The coupling path of the common mode noise current is shown in Fig. 6. As shown in Fig. 7, the differential mode noise current is mainly produced by the high frequency switching currents and the loops formed by the rectifier diodes and filter capacitors.

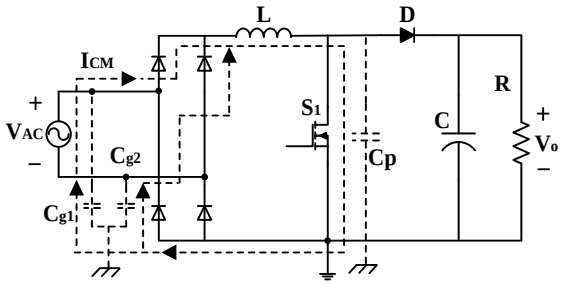

Fig. 6. The coupling path of the common mode noise current in PFC

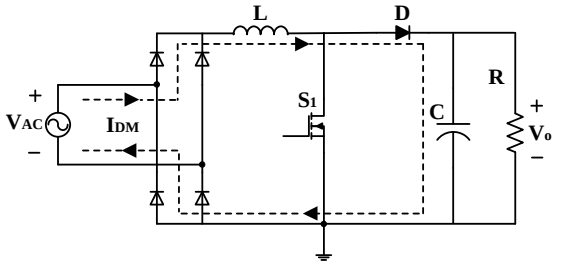

Fig. 7. The coupling path of the differential mode noise current in PFC

3.2 Electromagnetic Interference Standards and Specifications

Along with the fast development of high frequency power converters, every industrial country in the world has established its own electromagnetic compatibility (EMC) standards. The scope of EMC standards may technically includes relevant items in electromagnetic interference (EMI) and electromagnetic sensibility (EMS). At present, the most widely used EMC standards are mainly announced by the IEC and the CISPR. Since this paper is aimed to deal with the design issues of EMI filter for attenuating the conductive electromagnetic interference in active PFC circuits, only the standards regarding conducting EMI are briefly reviewed in the following part of this subsection.

In the United States, the standard, FCC 47 CFR Part 15 Subpart B (2007), provides EMI guidelines to two classes of electronic products, i.e. the Class A is set for products used in the commercial and industrial areas and the Class B is for products utilized in residential area. The test band of noises is from 150 kHz to30 MHz. The standard, EN55022, is widely referred in Europe. There are two categories of products, i.e., the industrial and residential applications of electronic products, covered in the regulation. The test band is also from 150kHz to 30MHz. In Taiwan, the CNS 13438 (Revised Edition) has been used as an official EMI standard which covers two types of application fields, i.e., the Class A is for electronic products used in the commercial and industrial areas, and the Class B is for products applied in residential area. The testing band is from 150kHz to 30MHz. The related limits are listed in Table 1.

Table 1. The conductive EMI limits (CNS 13438)

Frequency (MHz)	Class A		Class B	
	Limit (dBμV)		Limit (dBμV)	
	QP	AVG	QP	AVG
0.15~0.5	79	66	66~56	56~46
0.5~5.0	73	60	56	46
5.0~30	73	60	60	50

4. THE CONDUCTIVE EMI FILTER FOR PFC AND THE DESIGN STEPS

4.1 The Conductive EMI Filter

In this paper, the conventional EMI filter shown in Fig. 8 is used to demonstrate the proposed design method of the EMI filter to be cascaded with a digitally controlled boost PFC converter.

As shown in Fig. 8, there are two common mode inductors designed with high-μ ferrite cores to

meet the requirement of high inductance feature. The typical value is ranging from several mH to tens of mH. For the two differential mode inductors, the low-μ type of iron cores are used to have lower inductance feature and to allow flowing through the input line currents without too much voltage drop. The typical values of the differential mode inductors are between tens to hundreds of μH. As can be seen in Fig. 8, three X capacitors are connected between the Line and Neutral. These X capacitors have high capacitance and are generally the metal coating capacitors. The typical capacitance values are between 0.1 μF to 1 μF. The two Y capacitors are mounted between Line and Ground or Neutral and Ground. These Y capacitors usually designed in pairs and their sizes must be carefully chosen to comply with the limits of safety regulations. It should be noted that the Y capacitors could induce extra electrical leakage currents. Therefore in practical application cases, Y capacitors should not be too large. They are usually smaller than the X capacitors.

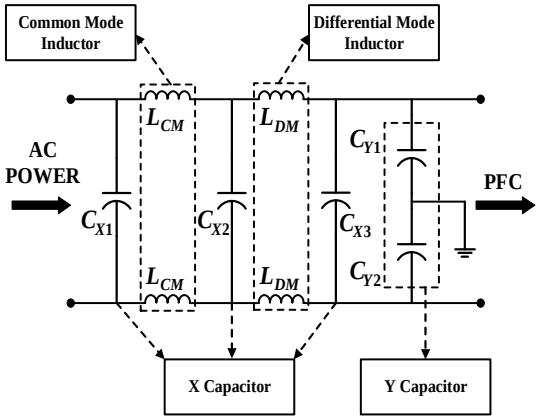

Fig. 8. The circuit of a conventional EMI filter

4.2 The Design Steps of a Conductive EMI Filter

In Taiwan, the compliance with CNS 13438 standard is one of the most important quality factors for designing power converters. In general, the design of EMI filter has to consider the whole power converter system and is split into radiated and conductive EMI considerations; however, for the PFC circuit investigated in this paper, it is most important to investigate on the conducted EMI-behavior since it is the input stage of any AC-DC power converters. The proposed design steps of a conductive EMI filter for a boost PFC circuit is given in the following.

Step 1: Measuring the original common mode and differential mode noises

In order to accurately design a filter, the measuring of original common mode and differential mode noises is the first step. This can be done by using a line impedance stabilization network (LISN), a noise separator and a spectrum analyzer [22] as shown in Fig. 9.

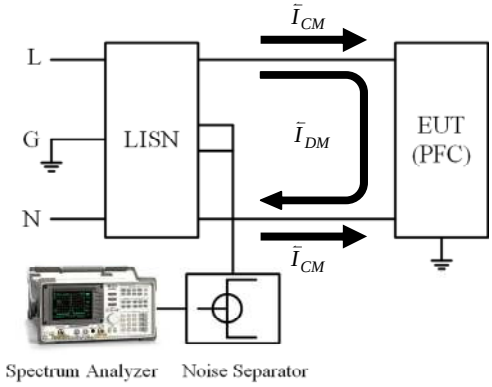

Fig. 9. The system setup for measuring conductive EMI noises

Step 2: Calculation of the required attenuation for the compliance with CNS 13438 standard.

After obtaining the original common mode and differential mode noise in step 1, the amount of filter attenuation can be determined with the CNS 13438 standard. The required attenuation targets of common mode and differential mode of the EMI filter can be calculated as:

$$V_{CM(Att,req)} = V_{CM(Act)} - V_{Limit} + 6dB \quad (10)$$

$$V_{DM(Att,req)} = V_{DM(Act)} - V_{Limit} + 6dB \quad (11)$$

In the above (10) and (11), $V_{CM(Act)}$ and $V_{DM(Act)}$ are the original common mode and differential mode noises obtained in step 1, V_{Limit} is the mean value of the standards referred. It should be noted that there is a 6dB added to the attenuation targets and to be considered as the safety margin to compensate the possible measuring errors.

Step 3: Calculation of corner frequencies of the EMI filter.

Using the spectrum data of the original common mode and differential mode noises and the

required attenuation quantities, $V_{CM(Att,req)}$ and $V_{DM(Att,req)}$, respectively obtained in the above step 1 and 2, the corner frequencies corresponding to the common mode/differential mode low-pass filters frequency $f_{R,CM}$ / $f_{R,DM}$ can be obtained by using two-dimensional mapping method with the unit of the horizontal axis in Hz and the dBμV for the vertical axis.

Step 4: Calculation of the parameters for the EMI filter.

According to the corner frequencies found in step 3, the related EMI filter elements, i.e. the inductance and capacitance values in Fig. 8 can be obtained using the following equations.

$$f_{R,CM} = \frac{1}{2\pi\sqrt{L_{CM} \cdot 2C_Y}} \quad (12)$$

$$f_{R,DM} = \frac{1}{2\pi\sqrt{2L_{DM} \cdot C_X}} \quad (13)$$

In the above (12) and (13), the L_{CM} and L_{DM} are respectively the common mode and differential mode inductances, C_X and C_Y are the corresponding capacitances. In practice, the capacitors must be chosen first based on a given leakage current specification and also considering the commercial availability. Then the inductors can be calculated with (12) and (13).

4.3 The Design Case and Quantitative Results

In this paper, the single-switch boost PFC circuit described in section 2 is taken as an example to test the effectiveness of the designed EMI filters. The design specifications of the PFC circuit are given in Table 2. The related EMI limits are referred to Table 1.

Table 2. The design specifications of the boost PFC

System parameters	Specifications
Input voltage	AC 110 V
output voltage	DC 390 V
Power frequency	60 Hz
Switching frequency	65 kHz
Rated power	1000 W
Load type	Resistive

According to the related regulations on leakage currents in Taiwan's low voltage distribution systems, the Y capacitors cannot exceed 3300 pF. In the design case, two capacitors with 2200 pF and 3300 pF are tested. With the corner frequency of the common mode filter to be 40 kHz, the corresponding common mode inductances are 3.6 mH and 2.4 mH respectively. For choosing the differential mode components, the X capacitance is normally ranging from 0.1 μF to 0.47 μF. Here, four values, 0.1 μF, 0.22 μF, 0.33 μF and 0.47 μF are selected for the X capacitors. For a corner frequency of differential mode filter to be 12 kHz, the corresponding differential mode inductances are 0.88 mH, 0.4 mH, 0.267 mH and 0.187 mH respectively. Using the above parameters, there are eight sets of unique EMI filters, as shown in Table 3. After the parameters of EMI filters are found, one can evaluate the performance of the individual EMI filter working with the boost PFC converter.

Table 3. Eight sets of EMI filters

Sets	Element			
	Common mode		Differential mode	
	L_{CM}	C_Y	L_{DM}	C_X
Set 1	3.6 mH	2200 pF	0.88 mH	0.1 μF
Set 2	3.6 mH	2200 pF	0.4 mH	0.22 μF
Set 3	3.6 mH	2200 pF	0.267 mH	0.33 μF
Set 4	3.6 mH	2200 pF	0.187 mH	0.47 μF
Set 5	2.4 mH	3300 pF	0.88 mH	0.1 μF
Set 6	2.4 mH	3300 pF	0.4 mH	0.22 μF
Set 7	2.4 mH	3300 pF	0.267 mH	0.33 μF
Set 8	2.4 mH	3300 pF	0.187 mH	0.47 μF

5. SIMULATION AND EXPERIMENTAL TEST RESULTS

5.1 Simulation and Results

In this section, the single-switch boost PFC presented in section 2 along with the designed EMI filters are developed and implemented in the PSIM software environment as shown in Fig. 10. The purpose of this simulation study is to evaluate the effectiveness of different combination of EMI parameters and the digital control strategies for the boost PFC circuit in terms of power factor correction and the current harmonic distortion. Simulation results are presented on different load levels, i.e. full load and half load. Two sets of simulation results on eight EMI parameters are respectively listed in Tables 4 and 5. Figs. 11 and 12 show the simulation results using the sixth set of EMI parameters in Table 3 which exhibits the best filtering results. Fig. 11(a) shows the simulation results of the input AC voltage and line current waveforms, power factor and the THD value for a half load (500 W) condition without EMI filter. Fig. 11(b) shows the corresponding output DC

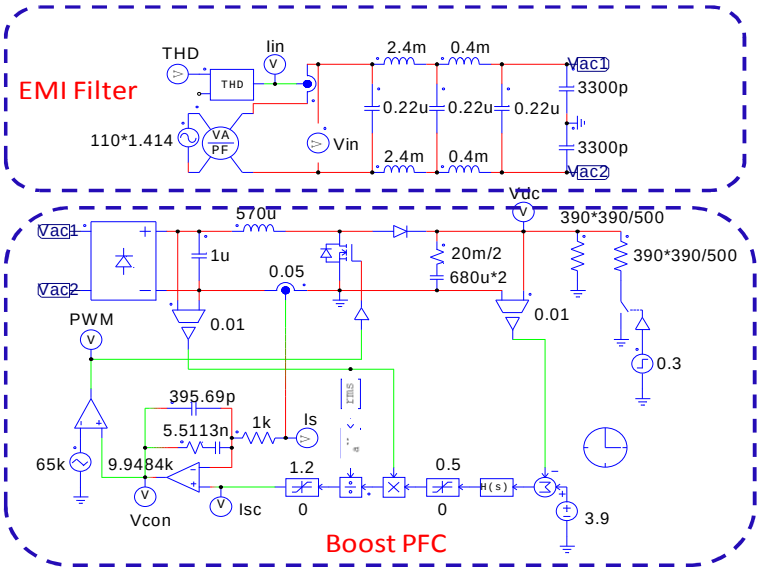

Fig. 10. The PSIM model of the single-switch boost PFC with an EMI filter

voltage, the current command and the sensed inductor current waveforms. Fig. 12(a) shows the simulation results of the input AC voltage and line current waveforms, power factor and the THD value for a half load (500W) condition with EMI filter. Fig. 12(b) shows the corresponding output DC voltage, the current command and the sensed inductor current waveforms with EMI filter. Fig. 13(a), (b) and Fig. 14(a), (b) respectively show the same waveform information as that presented in Fig. 11(a), (b) and Fig. 12(a), (b) except that the load level has been increased to 1 kW.

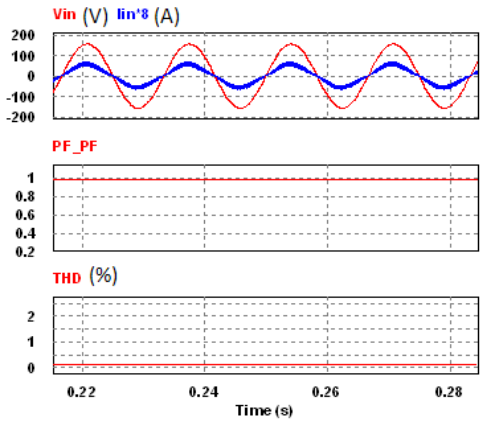

Fig. 11(a). The AC input voltage, line current waveforms, power factor and the THD values (500W, without EMI)

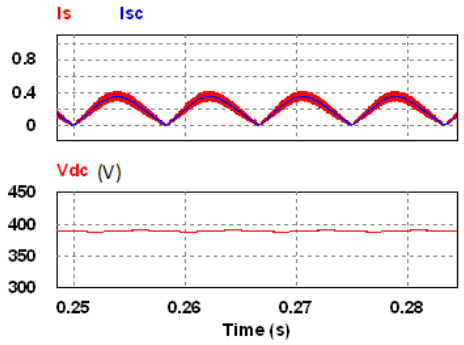

Fig. 11(b). The current command, the sensed inductor current waveforms and the output DC voltage (500W, without EMI)

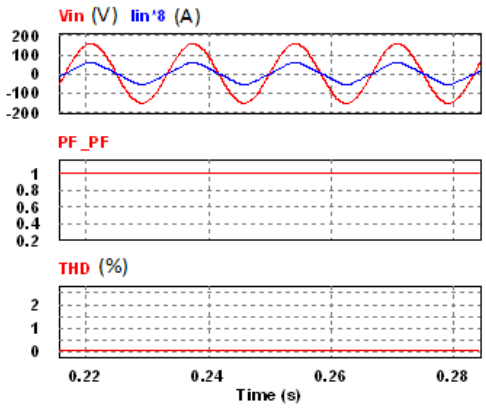

Fig. 12(a). The AC input voltage, line current waveforms, power factor and the THD value (500W, with EMI)

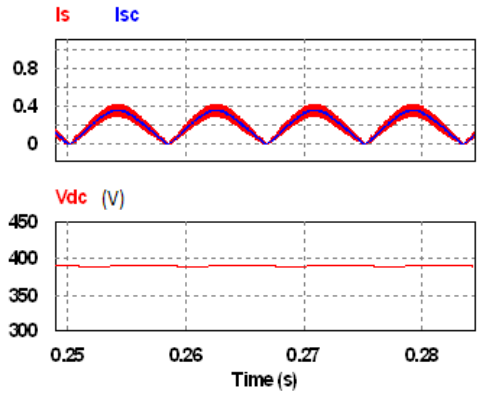

Fig. 12(b). The current command, the sensed inductor current waveforms and the output DC voltage (500 W, with EMI)

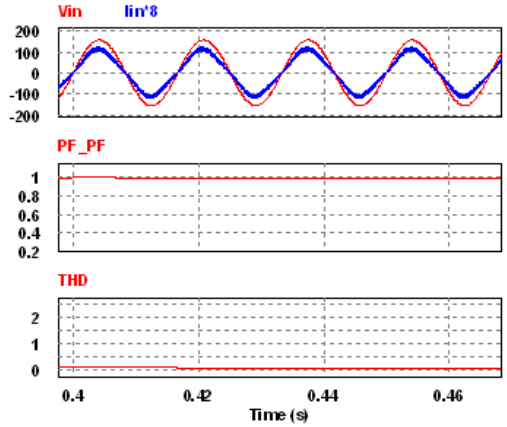

Fig. 13(a). The AC input voltage, line current waveforms, power factor and the THD values (1kW, without EMI)

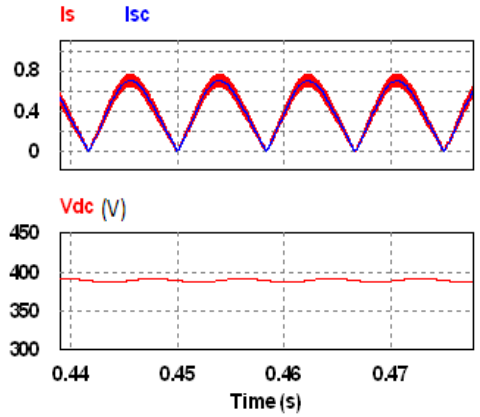

Fig. 13(b). The current command, the sensed inductor current waveforms and the output DC voltage (1 kW, without EMI)

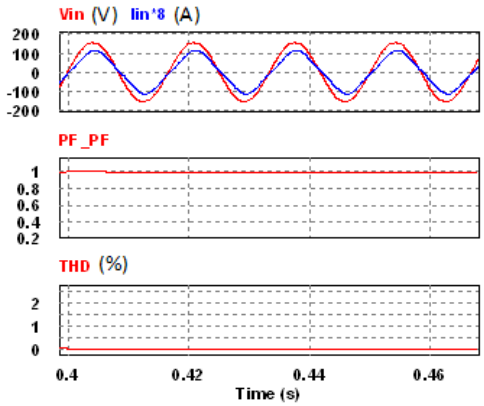

Fig. 14(a). The AC input voltage, line current waveforms, power factor and the THD values (1 kW, with EMI)

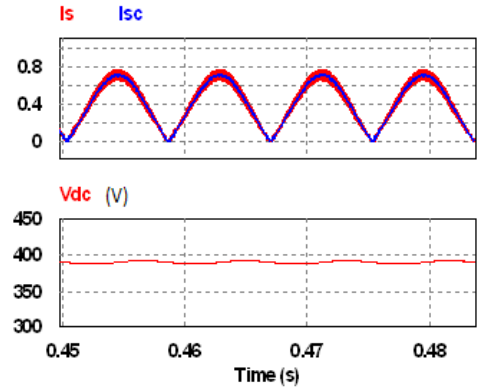

Fig. 14(b). The current command, the sensed inductor current waveforms and the output DC voltage (1 kW, with EMI)

Based on the simulation results, without EMI filter the PFC circuit has a simulated power factor of 0.961 and 0.97 and the THD of 21.34 and 12.26 respectively for half and full load conditions. As can be seen in Tables 4 and 5, the power factor can be raised up to 0.988 or even close to unity when the designed EMI filter is added. It is also found that in all cases, the total harmonic distortion (THD) can be greatly improved and are below 5%. Because the filter with the sixth set of parameters has the best overall performance the set of parameters are to be used in the hardware implementation and experimental tests presented in the next subsection.

5.2 Experimental Test and Results

To practically evaluate the performance of the designed EMI filters in terms of common mode

and differential mode noise-immunity, a 1kW boost PFC hardware prototype circuit controlled by a DSP (TMS320F28335) is constructed. The system specifications are the same as that modeled in PSIM model and listed in Table 2. Fig. 15 is the photo of the PFC hardware circuit and the test environment. Fig. 16 shows the CNS 13438 and the measured noise spectra of the boost PFC converter with the designed EMI filter. Fig. 17(a) shows the measured results of the input AC voltage and line current waveforms for a half load (500 W) condition without EMI filter. Fig. 17(b) shows the measured results of the input AC voltage and line current waveforms for a half load (500 W) condition with the designed EMI filter. Fig. 18(a) and (b) respectively show two sets of measured input voltage and line current waveforms corresponding to with and without the design EMI filters in which the PFC system is operated at full load (1 kW).

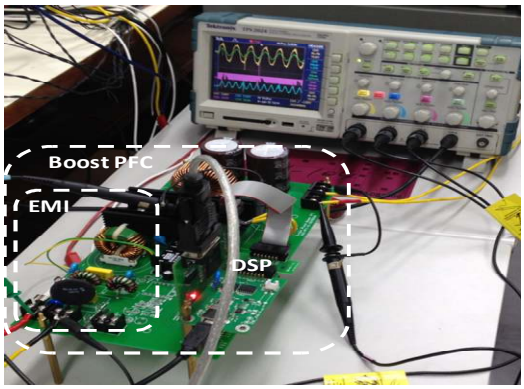

Fig. 15. Photo of the PFC circuit and test environment

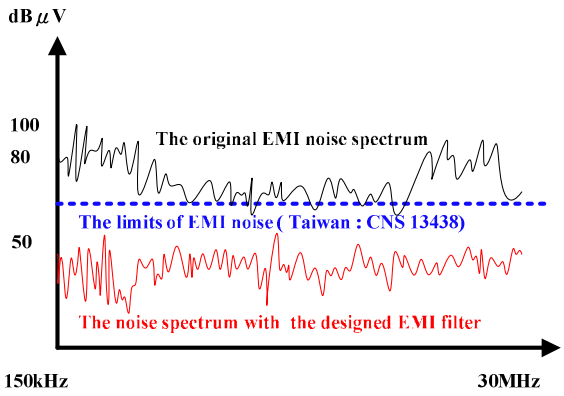

Fig. 16. The related noise spectra of the boost PFC converter with the designed EMI filter

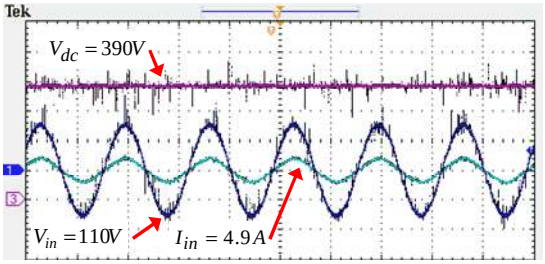

Fig. 17(a). The measured results of the input AC voltage and line current waveforms for a half load (500 W) condition without EMI filter

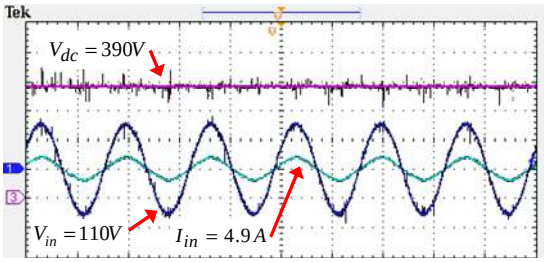

Fig. 17(b). The measured results of the input AC voltage and line current waveforms for a half load (500 W) condition with an EMI filter

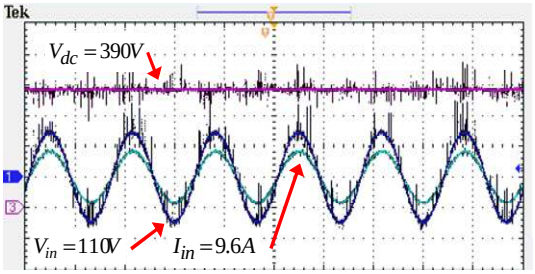

Fig. 18(a). The measured results of the input AC voltage and line current waveforms for a full load (1 kW) condition without EMI filter

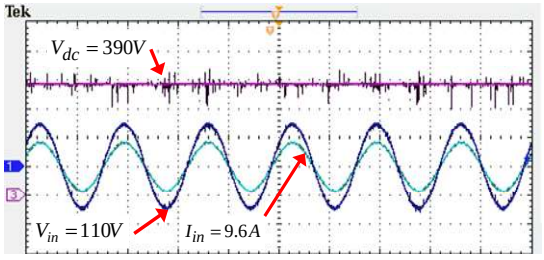

Fig. 18(b). The measured results of the input AC voltage and line current waveforms for a full load (1 kW) condition with an EMI filter

Table 4. Simulation results for half load

Parameters	Conditions: Half load (500 W)		
	Power factor	THD (%)	THD improved (%)
Without EMI	0.961	21.34	-
Set 1	0.997	4.92	16.38
Set 2	0.996	4.95	16.39
Set 3	0.996	4.65	16.69
Set 4	0.995	4.87	16.47
Set 5	0.996	4.81	16.53
Set 6	0.998	4.61	16.73
Set 7	0.995	4.72	16.73
Set 8	0.994	4.74	16.60

Table 5. Simulation results for full load

Parameters	Conditions: Full load (1kW)		
	Power factor	THD (%)	THD improved (%)
Without EMI	0.970	12.26	-
Set 1	0.982	3.91	8.35
Set 2	0.985	3.97	8.29
Set 3	0.986	3.74	8.52
Set 4	0.976	3.68	8.58
Set 5	0.985	3.52	8.74
Set 6	0.988	3.19	9.07
Set 7	0.977	3.23	9.03
Set 8	0.977	3.24	9.02

6. CONCLUSION

This paper has presented a quantitative design procedure for the EMI filters widely used in active PFC converters. A digitally controlled single-switch boost PFC converter and the issues regarding conductive EMI noises in terms of common-mode and differential mode characteristics exhibited in the PFC converter have been analyzed in detail. In this paper, a step by step EMI design procedure has been addressed along with the relevant international standards. It is important to note that the proposed design method is applicable for boost converters with other different topologies. To provide a simple guideline of choosing the best parameters for the EMI filters, a 1 kW DSP controlled boost converter has been chosen as a design example to test the effectiveness of the proposed EMI design method. The power factor and total harmonic distortion are taken as the main factors in evaluating the performance of the designed EMI filters. Comprehensive simulation studies in PSIM software environment have shown that there exist a number of different combinations of parameters providing satisfactory filtering effects on EMI noises; however, the best one can provide enough attenuation of noises without producing any leading-phase and ringing distortions. In this paper, a DSP based hardware prototype along with the designed EMI filter has been practically constructed and the effectiveness of the proposed design method has been verified with both simulation and measured results.

COMPETING INTERESTS

Authors have declared that no competing interests exist.

REFERENCES

1. Lv D, Zhang J, Dai Yu. Study on time and frequency-domain harmonic models of single-phase full bridge rectifiers. IEEE International Conference on Cyber Technology in Automation, Control, and Intelligent Systems (CYBER). 2015;1186-1198.
2. Mansouri M, Aghay Kaboli SH, Selvaraj J, Rahim NA. A review of single phase power factor correction A.C.-D.C. converters. IEEE Conference on Clean Energy and Technology (CEAT). 2013;389-394.
3. Umesh S, Venkatesha L, Usha A. Active power factor correction technique for single

phase full bridge rectifier. International Conference on Advances in Energy Conversion Technologies (ICAECT). 2014; 130-135.
4. Figueiredo JPM, Tofoli FL, Silva BLA. A review of single-phase PFC topologies based on the boost converter. 2010 9th IEEE/IAS International Conference on Industry Applications (INDUSCON). 2010; 1-6.
5. Liu Z, Lee FC, Li Q, Yang Y. Design of GaN-based MHz totem- broken PFC rectifier. 2015 IEEE Energy Conversion Congress and Exposition (ECCE). 2015; 682-688.
6. Xue L, Shen Z, Boroyevich D, Mattavelli P. GaN-based high frequency totem-pole bridgeless PFC design with digital implementation. 2015 IEEE Applied Power Electronics Conference and Exposition (APEC). 2015;759-766.
7. Zhou L, Wu Y, Honea J, Wang Z, High-efficiency true bridgeless totem pole PFC based on GaN HEMT: Design challenges and cost-effective solution. PCIM Europe. 2015;1-8.
8. Mao S, Ramabhadran R, Popovic J, Ferreira JA. Investigation of ccm boost PFC converter efficiency improvement with 600V wide band-gap power semiconductor devices. 2015 IEEE Energy Conversion Congress and Exposition (ECCE). 2015; 388-395.
9. Ji Q, Ruan X, Ye Z. The worst conducted EMI spectrum of critical conduction mode boost PFC converter. IEEE Transactions on Power Electronics. 2015;30(3):1230-1241.
10. Goswami R, Wang S, Chu Y. Modeling and analysis of hybrid differential mode filters for AC/DC converters to suppress current ripples and EMI. IEEE Energy Conversion Congress and Exposition (ECCE). 2015;2429-2436.
11. Liu Y, See KY, Tseng KJ. Conducted EMI prediction of the PFC converter including nonlinear behavior of boost inductor. IEEE Transactions on Electromagnetic Compatibility. 2013;55(6):1107-1114.
12. Ji Q, Ruan X, Xie L, Ye Z. Conducted EMI spectra of average-current-controlled boost PFC converters operating in both ccm and dcm. IEEE Transactions on Industrial Electronics. 2015;62(4):2184-2194.
13. Hamza D, Qiu M. Digital active EMI control technique for switch mode power converters. IEEE Transactions on Electromagnetic Compatibility. 2013;55(1): 81-88.
14. Yang F, Ruan X, Ji Q, Ye Z. Input differential-mode EMI of crm boost PFC converter. IEEE Transactions on Power Electronics. 2013;28(3):1177-1188.
15. Limits for Harmonic Current Emissions (Equipment Input Current < 16A per Phase), IEC/EN 61000-3-2; 1995.
16. IEEE standard conformance test procedures for equipment interconnecting distributed resources with electric power systems, IEEE Std 1547.1-2005; 2005.
17. EN-55022, European Standard of Limits for Harmonic Current Emissions; 2006.
18. FCC part 15B Test Report, Unilab (Shanghai), July 2013, Report No. UL15820130723FCC24-1.
19. Sankarl S, Padmarasan M, Raghavi T, Srishtisinha, Kumar SS. Simulation and design of closed loop controlled PFC boost converter with EMI filter. 2013 7th International Conference on Intelligent Systems and Control (ISCO). 2013;3-6.
20. Lim SB, Otten DM, Perreault JD. New AC–DC power factor correction architecture suitable for high-frequency operation. IEEE Transactions on Power Electronics. 2016; 31(4):2937-2949.
21. Chu YB, Wan S, Wang QH. Modeling and stability analysis of active/hybrid common-mode EMI filters for DC/DC power converters. IEEE Transactions on Power Electronics. 2016;31(9):6254-6263.
22. Tang YC, Chen JS, Lee CH, Chiu CN. A case study on the consistency improvement in radiated-emission testing by using LISN. International Symposium on Electromagnetic Compatibility, Tokyo (EMC'14/Tokyo). 2014;259-262.

Peer-review history:
The peer review history for this paper can be accessed here:
http://sciencedomain.org/review-history/14593